Adaptive control of dynamical synchronization on evolving networks with noise disturbances

Wu-Jie Yuan,[1,2,*] Jian-Fang Zhou,[1] Irene Sendiña-Nadal,[3,4] Stefano Boccaletti,[5] and Zhen Wang[6,†]
[1]*College of Physics and Electronic Information, Huaibei Normal University, Huaibei 235000, China*
[2]*College of Information, Huaibei Normal University, Huaibei 235000, China*
[3]*Complex Systems Group & GISC, Universidad Rey Juan Carlos, 28933 Móstoles, Madrid, Spain*
[4]*Center for Biomedical Technology, Universidad Politécnica de Madrid, 28223 Pozuelo de Alarcón, Madrid, Spain*
[5]*CNR-Institute of Complex Systems, Via Madonna del Piano, 10, 50019 Sesto Fiorentino, Florence, Italy*
[6]*School of Mechanical Engineering and Center for OPTical IMagery Analysis and Learning (OPTIMAL), Northwestern Polytechnical University, Xi'an, 710072, Shaanxi, China*

(Received 22 August 2017; revised manuscript received 27 January 2018; published 9 February 2018)

In real-world networked systems, the underlying structure is often affected by external and internal unforeseen factors, making its evolution typically inaccessible. An adaptive strategy was introduced for maintaining synchronization on unpredictably evolving networks [Sorrentino and Ott, Phys. Rev. Lett. **100**, 114101 (2008)], which yet does not consider the noise disturbances widely existing in networks' environments. We provide here strategies to control dynamical synchronization on slowly and unpredictably evolving networks subjected to noise disturbances which are observed at the node and at the communication channel level. With our strategy, the nodes' coupling strength is adaptively adjusted with the aim of controlling synchronization, and according only to their received signal and noise disturbances. We first provide a theoretical analysis of the control scheme by introducing an error potential function to seek for the minimization of the synchronization error. Then, we show numerical experiments which verify our theoretical results. In particular, it is found that our adaptive strategy is effective even for the case in which the dynamics of the uncontrolled network would be explosive (i.e., the states of all the nodes would diverge to infinity).

DOI: 10.1103/PhysRevE.97.022211

I. INTRODUCTION

Many real-world systems can be represented as complex networks [1–3], where nodes are dynamical systems that may organize to display collective and emergent dynamics, as for instance synchronization. Since Pecora and Carroll introduced the "Master Stability function" approach for the assessment of stability of the synchronous motion of units in a graph [4], many studies followed and extended that theory [3]. Network-mediated synchronization has today many applications in different fields, such as biological systems and neuroscience, engineering and computer science, or economy and social sciences. Imposing a synchronous behavior by judicious interventions (or controlling synchrony whenever it is lost) may be, therefore, sometimes desirable. However, a challenging problem of today's science is still finding the way to properly and effectively control the dynamical evolution of a distributed, networked, system [5–7].

Following studies on adaptive networks (i.e., on graphs where an interplay between structure and dynamics is explicitly taken into account [8,9]), strategies to pursue network synchronization have been proposed in which the coupling strengths are adaptively adjusted, based on some information about the nodes' dynamical state [10–14]. However, most of those strategies do not reflect the evolution of the connectivity commonly observed in many real-world networks [12,15,16]. For instance, the topology of wireless networks is constantly changing on the fly, in order to perform a given task or due to unforeseen numerous external and internal factors.

As the network structure evolves, the synchronized state one wants to target can be even destroyed, as network structure strongly impacts the stability of the dynamical synchronization [4]. The control strategies introduced so far, as for instance pinning control [17–20] and adaptive pinning control [21,22], rely on having access to some knowledge of the network topology. It is crucial to address the problem of control in evolving networks, and especially when information on the evolution of the network structure is not accessible. In Ref. [15], a first attempt was given for maintaining synchronization in a time varying network, which however does not consider unpredictable noise disturbances, which instead are typically present in a network environment [23,24].

In general, both intrinsic noise sources affecting each single unit of a network and communication noise affecting signal transmission over the network links [23,24] are unavoidable, and both sources of uncertainty should be simultaneously considered in the study of realistic networks. In our paper, we then provide an adaptive strategy to control dynamical synchronization on slowly evolving networks, under the explicit presence of such a type of fluctuations and under the explicit condition that the information on the graph structure is unavailable. In contrast with Ref. [15] (where only network changes were considered), we here try explicitly to cope with situations where two kinds of noise disturbances occur

*yuanwj2005@163.com
†zhenwang0@gmail.com

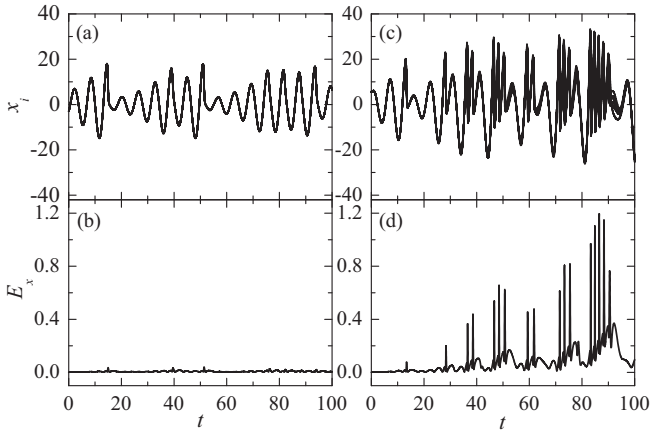

FIG. 1. (a) Time evolution of the x variable of eight randomly chosen nodes and (b) synchronization error in a random network with the Rössler model as the node dynamics, by using the adaptive strategy defined in Eq. (15). For comparison, panels (c) and (d) show the same quantities of panels (a) and (b), respectively, but calculated in the case of the fully nonadaptive strategy [i.e, $\sigma_i(t) \equiv \gamma / V_i(0)$]. Parameter values are the following: $N = 50$, $\langle k \rangle = 10$, $\gamma = 2.0$, $D = 0.5$, $C = 0.5$, $B_{1i}(0) = 10^4$, $B_{5i}(0) = 0$, $B_{4i}(0) = B_{1i}(0)/V_i(0)$, and $\nu = 1/1.4$.

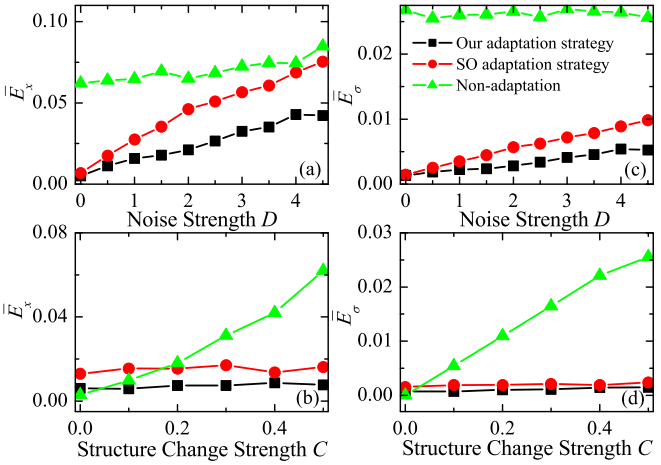

FIG. 2. (a), (b) Time average synchronization error $\bar{E}_x$, and (c), (d) the adaptation tracking error $\bar{E}_\sigma$ as a function of the noise intensity D (a), (c) and the structure change strength C (b), (d) for three different adaptive strategies: the method proposed in our paper, the SO strategy in Ref. [15], and a fully nonadaptive strategy (see legends for color codes). Each point is an average of 20 network realizations and initial conditions. The parameters are given by $C = 0.5$ in (a), (c) and $D = 0.5$ in (b), (d). Other parameters are the same as in the caption of Fig. 1.

simultaneously in the network. The nodes' coupling strength is adaptively adjusted according to their received signal and noise disturbances. Although the separation of noise from the signals is a challenging task in experimental realizations, our aim is just to point out that the adaptive control strategy is able, in principle, to outperform with respect to other, nonadaptive, control methods. In what follows, we will first describe the proposed control strategy (and give its detailed theoretical analysis) and then we will assess effectiveness of the proposed method by means of numerical simulations that fully verify the theoretical predictions.

II. ADAPTIVE STRATEGY

We here consider a network of dynamical units, where nodes are chaotic oscillators, and the coupling is in general a complex graph architecture. It is known that, in such conditions, an interesting interplay between individual and collective dynamics indeed takes place, and especially as far as synchronized collective behavior is concerned [3]. The dynamics under study refers to a generic weighted network, consisting in N identical coupled chaotic oscillators, and described by [3]

$$\dot{X}_i = F(X_i) + \frac{\gamma}{\sum_{j=1}^{N} G_{ij}} \sum_{j=1}^{N} G_{ij}[H(X_j) - H(X_i)]$$
$$= F(X_i) + \frac{\gamma}{V_i} \sum_{j=1}^{N} G_{ij} H(X_j) - \gamma H(X_i), \qquad (1)$$

where $F(X)$ denotes the dynamics of each individual chaotic unit, $H(X)$ is the coupling function, and γ is a coupling parameter which is equal for all nodes in the network. Here $G = (G_{ij})$ is a real valued matrix, accounting for the weights of the network's connections. More precisely, $G_{ij} = 0$ if nodes i and j are not connected, $G_{ii} \equiv 0$ $(\forall i)$, and $G_{ij} \neq 0$ for each pair of connected units in the graph.

The communication (coupling) capacity of each node is likely to saturate when the number of nodes connected to it becomes too large [25]. For example, in neural systems, the transmitter resources of the vesicles responsible for the synaptic coupling strength in a neuron are invariant, no matter how many other neurons are connected through synapses. Therefore, the coupling matrix is here normalized by G_{ij}/V_i, where $V_i = \sum_{j=1}^{N} G_{ij}$ denotes the intensity (strength) of node i. While heterogeneity in the network topology or/and weights may eventually hamper synchronization when G_{ij} is regarded as a straight coupling matrix [26], when the normalization factor G_{ij}/V_i is accounted for, the graph's synchronizability can be instead enhanced [3].

Model (1) is not taking into account environmental noise, whose incorporation leads to

$$\dot{X}_i = F(X_i) + \frac{\gamma}{V_i} \sum_{j=1}^{N} G_{ij} H(X_j) - \gamma H(X_i)$$
$$+ K(U_i) + \sum_{j=1}^{N} G_{ij} K(U_j). \qquad (2)$$

Now, Eq. (2) includes a signal coupling term $\frac{\gamma}{V_i} \sum_{j=1}^{N} G_{ij} H(X_j) - \gamma H(X_i)$, and the noise term $K(U_i) + \sum_{j=1}^{N} G_{ij} K(U_j)$. Here $K(U_i)$ quantifies the effect of the intrinsic noise disturbance U_i occurring at node i, while $\sum_{j=1}^{N} G_{ij} K(U_j)$ accounts for the communication noise disturbance to node i from other connected nodes j.

In order to control (or maintain) synchronization, we consider a slowly time varying network in which the available external information at node i includes the signal

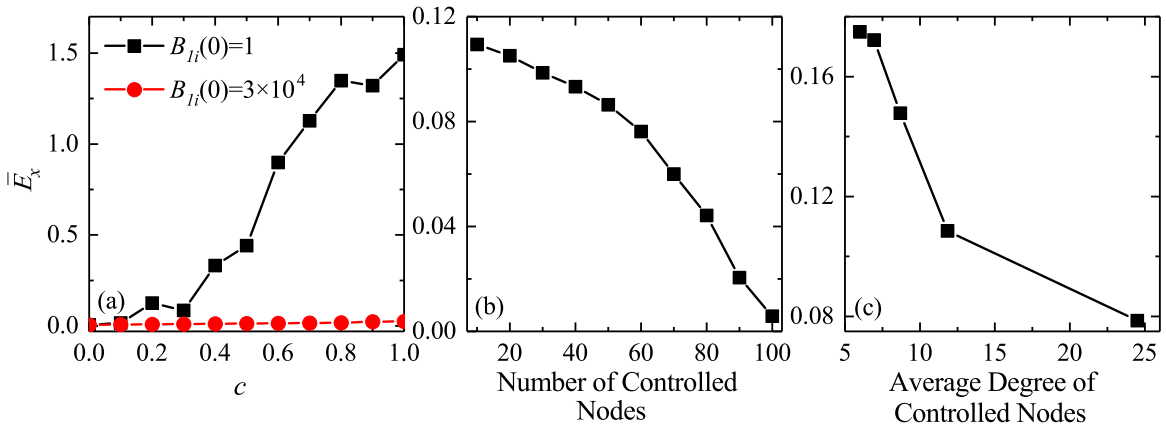

FIG. 3. Time average synchronization error $\bar{E}_x$ as a function of (a) the dispersion c in the initial conditions for two different initial values of $B_{1i}(0)$, (b) the number of controlled nodes, and (c) the average degree of the nodes being controlled. In panels (a) and (b) the network topology is random with a homogeneous degree distribution ($N = 100$ and $\langle k\rangle = 20$), and in panel (c) it is a BA scale-free network ($N = 100$ and $\langle k\rangle = 12$). Each point is an average over 20 network realizations and initial conditions. Other parameters are the same as in Fig. 1, except for the two different values $B_{1i}(0) = 1$ and $B_{1i}(0) = 3 \times 10^4$ in panel (a).

$S_i = \sum_{j=1}^{N} G_{ij} H(X_j)$ and the noise $\sum_{j=1}^{N} G_{ij} K(U_j)$ transmitted through the network connections, whereas direct knowledge of $V_i = \sum_{j=1}^{N} G_{ij}$ (that is, the network structure) is unavailable. For the purpose of our adaptive synchronization strategy, we assume that S_i is adaptively modified to reach a synchronous condition. The adaptive network can be described by

$$\dot{X}_i = F(X_i) + \sigma_i S_i - \gamma H(X_i) + M_i, \tag{3}$$

where σ_i is the coupling strength of the network signal S_i received by node i and $M_i = K(U_i) + \sum_{j=1}^{N} G_{ij} K(U_j)$ accounts for the total noise disturbances acting on node i. Assuming the network synchronous state to be described by $X_1(t) = X_2(t) = \cdots = X_N = X_s$, the sum of the last three terms in Eq. (3) is required to be identically zero. The synchronous dynamics is therefore governed by the equation describing the evolution of a single, isolated, system

$$\dot{X}_s = F(X_s). \tag{4}$$

According to Eq. (1), in the time varying network without noise disturbances, the synchronous solution exists if all σ_i adaptively evolve as

$$\bar{\sigma}_i(t) = \frac{\gamma}{V_i(t)}, \tag{5}$$

as reported in Ref. [15]. Reference [4] introduced a powerful method to assess synchronization stability of networked oscillators (for any linear coupling) by the use of the master stability function. The same arguments apply for our adaptive model and the stability of the synchronous evolution depends essentially on the choice of an appropriate coupling γ. We start by choosing an adequate value of γ, for which the synchronous state is stable in the absence of noise and in a static network. When $\sigma_i(t)$ is changed by Eq. (5), then the adaptive scheme admits in general a stable synchronous solution [15]. Here, we focus only on the maintenance of synchronization for low values of additional noise intensities. In order to better monitor the case of a time varying network with noise disturbances, our contribution is to control the time evolution of $\sigma_i(t)$ so that the sum of the last three terms in Eq. (3) tends to relax toward zero. To that purpose, we define a mean squared exponentially weighted synchronization error (as a potential error function) for each node i,

$$\Delta_i(t) = \int_0^t e^{-\nu(t-t')} |\sigma_i(t') S_i(t') - \gamma H(X_i(t')) + M_i(t')|^2 dt', \tag{6}$$

where ν^{-1} denotes the temporal extent over which the averaging synchronization error is performed.

Here, we consider the case in which the time scale τ_S of the node dynamics $X_i(t)$ is much smaller than the time scale τ_N for the evolution of network structure $G_{ij}(t)$ [i.e., the time scale on which V_i and hence $\bar{\sigma}_i(t)$ change]. The value of ν^{-1} will be chosen such that $\tau_S < \nu^{-1} < \tau_N$. Following this assumption, one can replace $\sigma_i(t')$ in Eq. (6) by $\sigma_i(t)$, which can be approximated as

$$\begin{aligned}\Delta_i(t) &\approx \int_0^t e^{-\nu(t-t')} |\sigma_i(t) S_i(t') - \gamma H(X_i(t')) + M_i(t')|^2 dt' \\ &= \sigma_i^2(t) B_{1i}(t) + \gamma^2 B_{2i}(t) + B_{3i}(t) \\ &\quad - 2\gamma\sigma_i(t) B_{4i}(t) + 2\sigma_i(t) B_{5i}(t) - 2\gamma B_{6i}(t),\end{aligned} \tag{7}$$

where

$$B_{1i}(t) = \int_0^t e^{-\nu(t-t')} S_i^2(t') dt', \tag{8}$$

$$B_{2i}(t) = \int_0^t e^{-\nu(t-t')} H^2(X_i(t')) dt', \tag{9}$$

$$B_{3i}(t) = \int_0^t e^{-\nu(t-t')} M_i^2(t') dt', \tag{10}$$

$$B_{4i}(t) = \int_0^t e^{-\nu(t-t')} S_i(t') H(X_i(t')) dt', \tag{11}$$

$$B_{5i}(t) = \int_0^t e^{-\nu(t-t')} S_i(t') M_i(t') dt', \tag{12}$$

and

$$B_{6i}(t) = \int_0^t e^{-\nu(t-t')} H(X_i(t')) M_i(t') dt'. \tag{13}$$

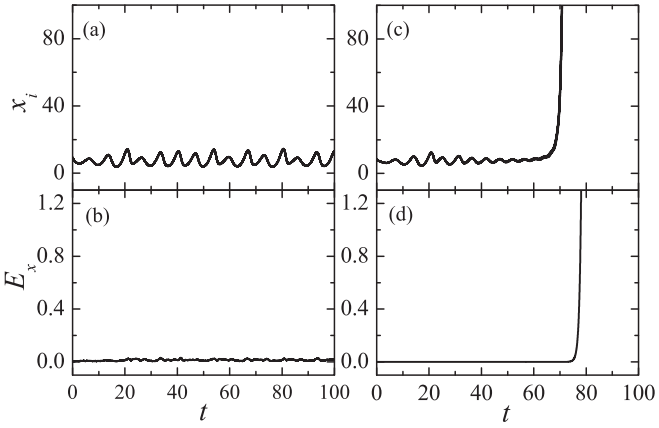

FIG. 4. (a) Time evolution of the x variable of eight randomly chosen nodes and (b) synchronization error in the presence of noise, for the Foodweb model. For comparison, panels (c) and (d) show the same quantities of panels (a) and (b), respectively, but calculated in the case of a fully nonadaptive strategy. In panel (c) it is shown that the network is explosive for the case of a nonadaptive strategy and the states of all the nodes tend to infinity. Parameter values are $N = 50$, $\langle k\rangle = 10$, $\gamma = 2.0$, $D = 0.5$, $C = 0.5$, $B_{1i}(0) = 10^4$, $B_{5i}(0) = 0$, $B_{4i}(0) = B_{1i}(0)/V_i(0)$, and $\nu = 1/1.4$.

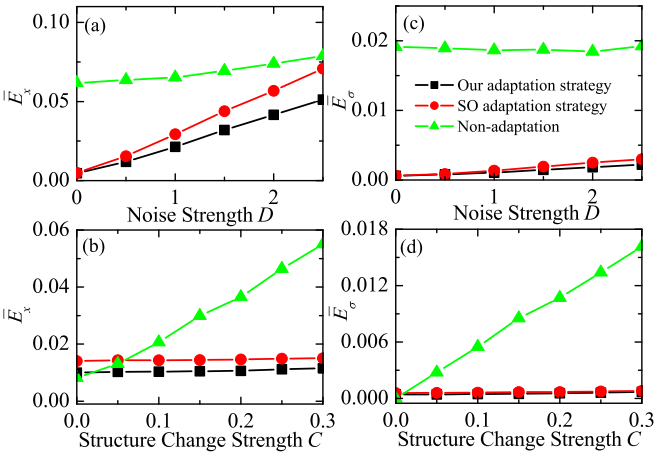

FIG. 5. (a), (b) Time average synchronization error $\bar{E}_x$ and (c), (d) the adaptation tracking error $\bar{E}_\sigma$ as a function of the noise intensity D (a), (c) and the structure change strength C (b), (d) for the Foodweb model and three different adaptive strategies: the method proposed in our paper, the SO strategy, and a fully nonadaptive strategy (see legends for color codes). Each point is an average of 20 network realizations and initial conditions. $C = 0.35$ in (a), (c) and $D = 0.5$ in (b), (d). Other parameters as in the caption of Fig. 4.

One way to engineer $\sigma_i(t)$ (to minimize the potential function Δ_i) is by the following gradient descent relaxation [15]:

$$\frac{d\sigma_i(t)}{dt} = -\alpha\frac{d\Delta_i}{d\sigma_i} = -2\alpha(\sigma_i B_{1i} - \gamma B_{4i} + B_{5i}), \tag{14}$$

where α denotes the relaxation time scale. Taking $\alpha \to +\infty$, one gets

$$\sigma_i(t) = \frac{\gamma B_{4i} - B_{5i}}{B_{1i}}. \tag{15}$$

To further simplify the calculation, one can transform the integrals (8), (11), and (12) into the following differential equations:

$$\frac{dB_{1i}(t)}{dt} = -\nu B_{1i} + S_i^2, \tag{16}$$

$$\frac{dB_{4i}(t)}{dt} = -\nu B_{4i} + S_i H(X_i), \tag{17}$$

$$\frac{dB_{5i}(t)}{dt} = -\nu B_{5i} + S_i M_i. \tag{18}$$

According to the above analysis, one thus gets an effective way for controlling network synchronization by means of Eqs. (3) and (15)–(18).

III. NUMERICAL EXPERIMENTS

To check for effectiveness of our adaptive strategy, we practically implement it on a random network of N nodes with mean degree $\langle k\rangle$, where each node is described by a chaotic Rössler oscillator [27]: $X = (x,y,z)$ and $F(X) = [-y - z, x + 0.165y, z(x - 10.0) + 0.2]$. For practical purposes, one assumes the following time dependence of the links' weights:

$$G_{ij} = 1 + C\varepsilon_{ij}\sin(\omega_{ij}t), \tag{19}$$

where ε_{ij} and ω_{ij} are chosen from uniform distributions (between 0 and 1 and between 0.01 and 0.02, respectively), and C stands for the amplitude of the modulation of the network weights' change.

For the sake of simplicity, one can consider the coupling and disturbing functions to be linear. This is tantamount to fixing $H(X) = HX$ and $K(U) = KU$. In particular, one can choose $H = K = [1\ 0\ 0;\ 0\ 0\ 0;\ 0\ 0\ 0]$ and $U_i = (D\mu_i\ 0\ 0)$, where $\mu_i(t)$ is a white noise of zero mean uniformly distributed between -0.5 and 0.5 and D is the noise intensity.

In all simulations, the network is in a synchronous state at $t = 0$ and the time synchronization error $E_x(t)$ is defined as

$$E_x(t) = \frac{1}{N\rho_x}\sum_{i=1}^{N} |\, x_i(t) - \bar{x}(t)\,|\,, \tag{20}$$

where $\bar{x}(t) = \frac{1}{N}\sum_{i=1}^{N} x_i(t)$ and ρ_x is the standard deviation of $\bar{x}(t)$, i.e., $\rho_x = [\frac{1}{t}\int_0^t \bar{x}^2(t')dt' - (\frac{1}{t}\int_0^t \bar{x}(t')dt')^2]^{1/2}$.

The results are shown in Fig. 1 and confirm that our adaptive strategy is able to maintain the initial synchronous state. In Fig. 1(a), in particular, one can see the coincidence of the trajectories of eight randomly chosen nodes in the network. In Fig. 1(b), the vanishing of the synchronization error $E_x(t)$ can be easily seen in the whole time window explored. It is found that the synchronization error remains always close to zero in the evolving network. For comparison, we also show in Figs. 1(c) and 1(d) the same case, where however the adaptive strategy is not implemented. There, the synchronous trajectory is instead abandoned and the synchronization error is getting larger and larger in the course of time.

A better understanding comes from exploring the effect that (i) the noise intensity D and (ii) the network parameter C have on the controllability of the network synchronization. Results are provided in Fig. 2, where we introduce an average

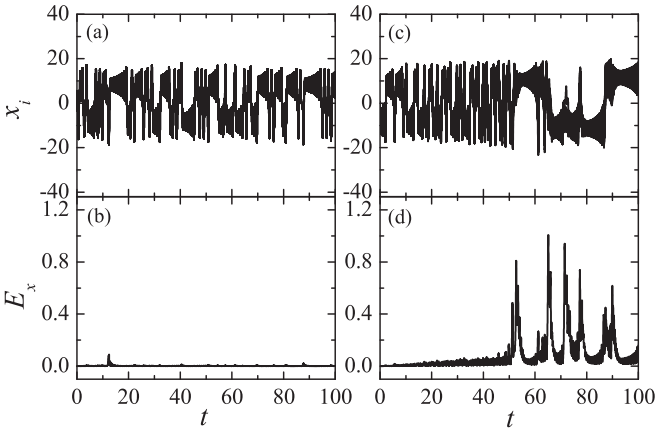

FIG. 6. Same quantities as in the caption of Fig. 4, but for Lorenz model. $\gamma = 20.0$, while the other parameters of the control method are the same as in the caption of Fig. 4.

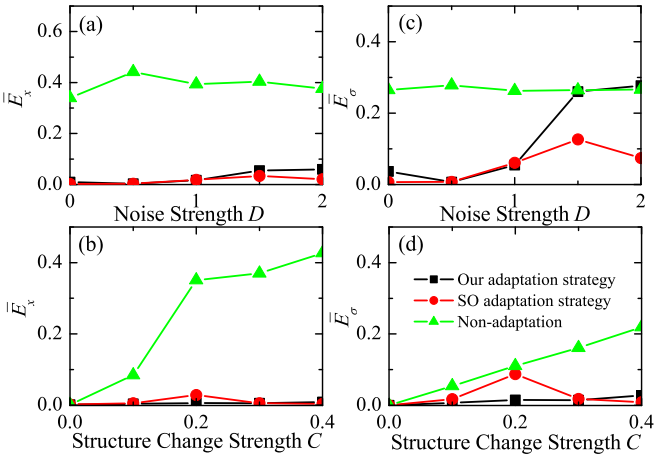

FIG. 7. Same quantities as in the caption of Fig. 5, but for Lorenz model. Parameter values are the same as in Fig. 5, except for $\gamma = 20.0$ and $C = 0.5$ in (a), (c).

synchronization error $\bar{E}_x$, defined as $\bar{E}_x = \frac{1}{t}\int_0^t E_x(t)dt$ and we compare our adaptive strategy [as described in Eq. (15)] with the Sorrentino and Ott (SO) adaptive method [as described by $\sigma_i(t) = \frac{\gamma B_{4i}}{B_{1i}}$ in Ref. [15]], as well as with a nonadaptive strategy [i.e, $\sigma_i(t) \equiv \frac{\gamma}{V_i(0)}$].

It is observed in Fig. 2(a) that the average synchronization error $\bar{E}_x$ increases as D increases (as expected in the three cases), but its value remains much lower when using the adaptive strategy proposed in this paper. On the other hand, when studying the impact of introducing a change in the network's links, the error remains bounded with the parameter C in the two adaptive cases, while it increases when a nonadaptive strategy is adopted [see Fig. 2(b)].

The success of the controlling scheme depends on the fact that $\sigma_i(t)$ keeps tracking the dynamics of $\bar{\sigma}_i(t)$. In order to verify this, one can define a tracking error,

$$\bar{E}_\sigma = \frac{1}{Nt}\int_0^t \sum_{i=1}^{N} \mid \sigma_i(t) - \bar{\sigma}_i(t) \mid dt. \qquad (21)$$

In Figs. 2(c) and 2(d) one sees that (in the presence of noise) our adaptive strategy is the best for tracking the state of $\bar{\sigma}_i(t)$. The tracking is instead totally lost when nonadaptive strategies are adopted. Moreover, one can see that both the synchronization error and the tracking error $\bar{E}_\sigma$ are in our case always smaller than those obtained by the use of the SO strategy, thus indicating that our method outperforms the SO one when one has to control synchronization on evolving networks with noise disturbances.

In the Appendix, the reader can find extensive numerical simulations, which verify our theoretical results in other three dimensional chaotic dynamics, such as the Foodweb model [28] and the Lorenz model [29]. Furthermore, our results are also verified with the Mackey-Glass equation [30,31], a time delay differential equation exhibiting high dimensional chaotic dynamics. The Appendix also displays results for a Rössler network with other linearly coupling functions. In particular, it is found that our adaptive strategy is effective even for the case in which the dynamics of the uncontrolled network would be explosive (i.e., the states of all the nodes would diverge to infinity).

We further address the issue of the robustness of the adaptive strategy in different scenarios. In the first one, we examine how robust is the control of the synchronous state against the choice of initial conditions for the state X_i and control B_{1i} variables. According to Ref. [15], when selecting the initial conditions for the state variables close to the basin of attraction of the targeted synchronous solution, one has $B_{1i}(0) \simeq \langle S_i^2 \rangle = \langle k^2 \rangle \langle x_s^2 \rangle$, with $\langle k^2 \rangle$ being the second moment of the degree distribution and $\langle x_s^2 \rangle$ the time average of $x_s(t)$ for the synchronous chaotic dynamics. For the case we are here considering (a random network of $N = 100$ Rössler oscillators coupled through the x variable and $\langle k \rangle = 20$), one has $B_{1i}(0) = 10^4$. In order to investigate how the setting of such an initial value depends on the $X_i(0)$ variables, we prepare the network state as $x_i(0) = x_0 + c\rho_x\epsilon_{ix}$, $y_i(0) = y_0 + c\rho_y\epsilon_{iy}$, and $z_i(0) = z_0 + c\rho_z|\epsilon_{iz}|$. In the latter expression (x_0, y_0, z_0) is a random point in the Rössler attractor; ϵ_{ix}, ϵ_{iy}, and ϵ_{iz} are random numbers taken from a normal distribution of zero mean and unit variance. Furthermore, $\rho_x = 7.45$, $\rho_y = 7.08$, and $\rho_z = 4.25$ are the standard deviations of the time evolutions of the synchronous states x_s, y_s, and z_s, and the parameter c reflects the degree to which the initial conditions vary among nodes.

Figure 3(a) compares the result at $B_{1i}(0) \simeq 10^4$ (3×10^4 is given) with that at $B_{1i}(0) = 1$. It is clearly seen that good synchronization is achieved when $B_{1i}(0) \simeq 10^4$ for different c values, whereas the network fails to synchronize as c increases above 0.1 when $B_{1i}(0) = 1$.

Finally, we investigate the impact of a *pinning* control strategy, which is limited to just a given percentage of the network's nodes. In a random network characterized by a homogeneous degree distribution, it is not surprising that the control becomes progressively more and more effective as the number of controlled (pinned) nodes increases, as shown in Fig. 3(b). In order to highlight the role of network heterogeneity, we apply our method to a Barabási-Albert (BA) scale-free network [32]. The procedure consists in ranking

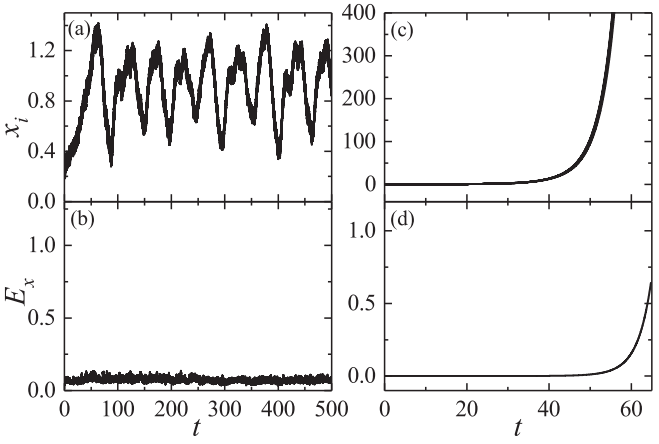

FIG. 8. Same quantities as in the caption of Fig. 4, but for Mackey-Glass chaotic dynamics. Panel (c) shows that the network is explosive for a nonadaptive control strategy. The parameter values are the same as in Fig. 4.

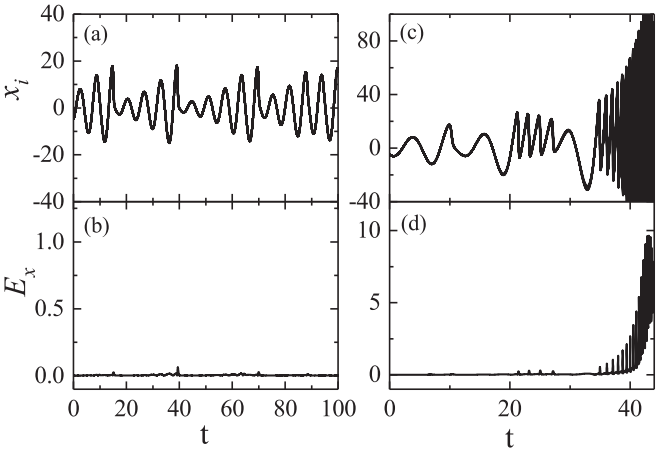

FIG. 10. Same quantities as in the caption of Fig. 4, but for Rössler oscillators networked with a coupling function $H = [1\ 0\ 0;\ 0\ 1\ 0;\ 0\ 0\ 0]$). Panel (c) shows that the network is explosive for the nonadaptive case. Parameter values are the same as in Fig. 4.

the nodes according to their degree and dividing them in five different communities, each community containing the 20% of the nodes. In other words, community one will contain the 20% of nodes with highest degree, community two will contain the second 20% of nodes in the degree ranking, etc., up to community five, which will contain the 20% of nodes of lowest degree. Then, the control is successively applied to each community. The results are summarized in Fig. 3(c), where one can observe that the synchronization error decreases as the average degree of each block of nodes increases, meaning that the adaptive strategy is more effective when applied to the hubs of the network.

IV. CONCLUSION AND DISCUSSION

In conclusion, we have introduced an effective strategy which controls synchronization on slowly evolving networks in the presence of noise disturbances and which accounts for both the intrinsic fluctuations at the single node level and the communication noise over the network connections. In our strategy, when the evolution of the network structure is unknown, the coupling strengths of nodes are adaptively adjusted for controlling network synchronization according only to their received input signal and noise disturbance from neighboring nodes. It is worth noticing that, in order to calculate the adaptive coupling, we need to have access to the noise source separately from the signal in real time. However, despite the fact that acquisition of noise is not a trivial task experimentally, some techniques for real-time separation of noise from signals are available today and, therefore, our control strategy could be used as long as the time scale of the

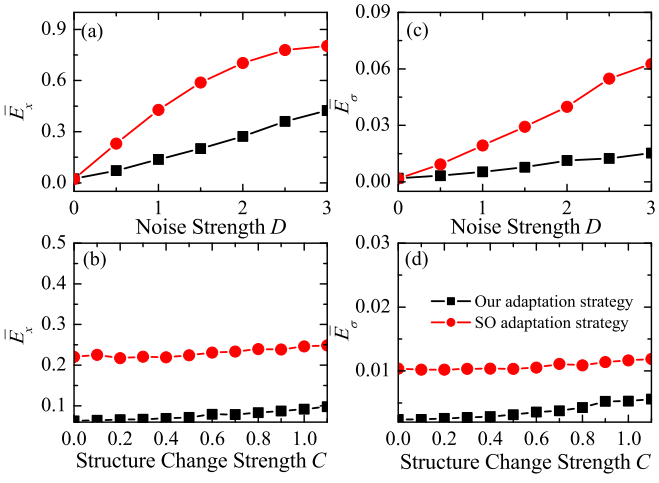

FIG. 9. Same quantities as in the caption of Fig. 5, but for Mackey-Glass chaotic dynamics. Here the case of nonadaptation is not shown, as the network is explosive there [see Fig. 8(c)]. Parameter values are the same as in Fig. 5, except for $C = 0.5$ in (a), (c).

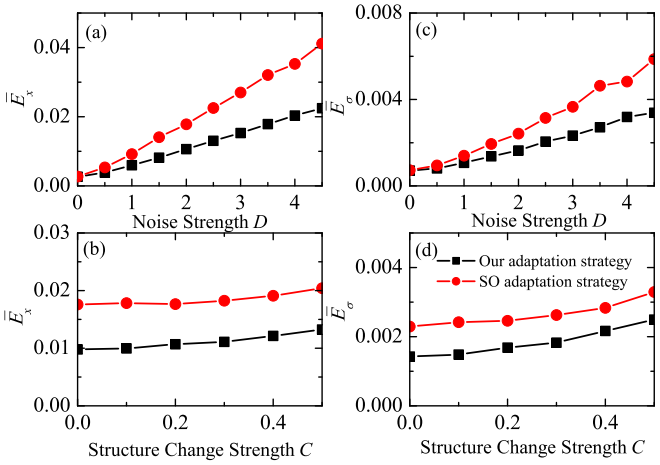

FIG. 11. Same quantities as in the caption of Fig. 5, but for Rössler oscillators networked with a coupling function $H = [1\ 0\ 0;\ 0\ 1\ 0;\ 0\ 0\ 0]$). The nonadaptive case is not shown, because the network is explosive there [see Fig. 10(c)]. Parameter values are the same as in Fig. 5, except for $C = 0.2$ in (a), (c) and $D = 2.0$ in (b), (d).

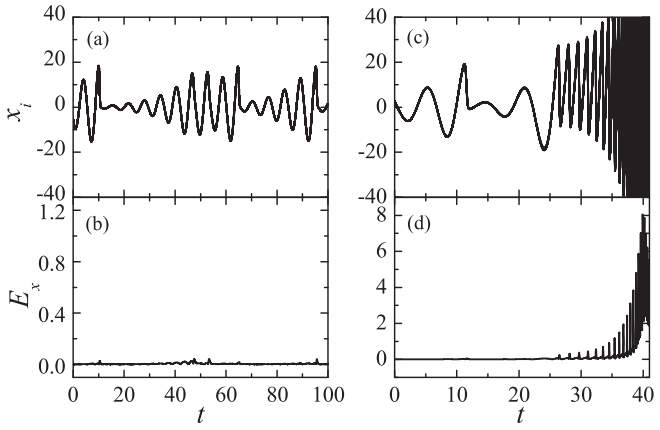

FIG. 12. Same quantities as in the caption of Fig. 4, but for Rössler oscillators networked with a coupling function $H = [1\ 0\ 0;\ 0\ 1\ 0;\ 0\ 0\ 1]$). Panel (c) shows that the network is explosive for the nonadaptive case. Parameter values are the same as in Fig. 4.

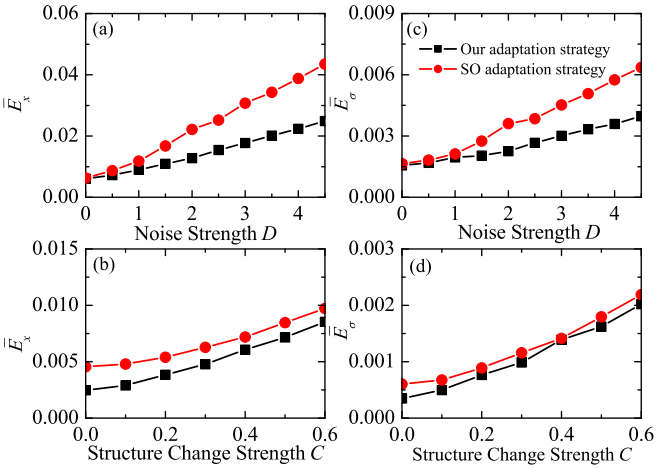

FIG. 13. Same quantities as in the caption of Fig. 5, but for Rössler oscillators networked with a coupling function $H = [1\ 0\ 0;\ 0\ 1\ 0;\ 0\ 0\ 1]$). The nonadaptive case is not shown, because the network is explosive there [see Fig. 12(c)]. Parameter values are the same as in Fig. 5, except for $C = 0.5$ in (a), (c).

dynamics to be controlled is slow enough to warrant real-time processing of the signal to extract the noise sources.

We not only give theoretical analysis, but also show numerical examples for verifying the effectiveness of our adaptation strategy. We deal with the issue of keeping a synchronous state in the presence of noise. It is found that our method outperforms with respect to the previous strategies considered in the literature [15], and as so it is a good candidate for applications in real world networked systems.

ACKNOWLEDGMENTS

This work is partially supported by Natural Science Foundation of Anhui Province under Grant No. 1508085MA04, Project of Natural Science in Anhui Provincial Colleges and Universities under Grants No. KJ2015ZD33 and No. KJ2016B006, Major Project of Outstanding Young Talent Support Program in Anhui Provincial Colleges and Universities under Grant No. gxyqZD2016410, the National 1000 Young Talent Plan W099102, the Fundamental Research Funds for the Central Universities G2017KY0001, CCF-Tencent IAGR20170119, and Scientific and Technological Activity Foundations for Preferred Overseas Chinese Scholar in Ministry of Human Resources and Social Security of China and in Department of Human Resources and Social Security of Anhui Province.

APPENDIX: EXTENSIVE NUMERICAL SIMULATIONS

In order to provide a verification of our theoretical results for the generic use of dynamical systems as network's nodes, we present here the results of extensive numerical simulations which were done with other three (or higher) dimensional chaotic dynamics.

The considered models (using the same notations as in the main text) are as follows.

(i) The Foodweb model: $F(X) = [x - 0.2xy/(1 + 0.05x), -y + 0.2xy/(1 + 0.05x) - yz, -10(z - 0.006) + yz]$ (the results are reported in Figs. 4 and 5).

(ii) The Lorenz model: $F(X) = [10(y - x), 28x - y - xz, xy - \frac{8}{3}z]$ (the results are reported in Figs. 6 and 7).

(iii) The Mackey-Glass equation (results reported in Figs. 8 and 9). This latter chaotic dynamics is the result of a time-delay ordinary differential equation: $\frac{dx(t)}{dt} = \frac{ax(t-\tau)}{1+x^{10}(t-\tau)} - bx(t)$. The system shows chaotic behavior when $\tau > 17$, and the dimensionality of its chaotic attractor is very well known to grow linearly with τ. In our simulations, we adopted $\tau = 18$, $a = 0.2$, and $b = 0.1$.

(iv) The same Rössler model as in the main text, but on networks with other linearly coupling functions: $H = [1\ 0\ 0;\ 0\ 1\ 0;\ 0\ 0\ 0]$) (results shown in Figs. 10 and 11) and $H = [1\ 0\ 0;\ 0\ 1\ 0;\ 0\ 0\ 1]$) (results reported in Figs. 12 and 13).

In all cases our adaptive strategy is extraordinarily effective. Remarkably, also when the dynamics of the uncontrolled network would be explosive [i.e., the states of all the nodes would diverge to infinity; see Figs. 4(c), 8(c), 10(c), and 12(c)], our method can successfully control synchronization [see Figs. 4(a), 8(a), 10(a), and 12(a)].

[1] R. Albert and A.-L. Barabási, Rev. Mod. Phys. **74**, 47 (2002).
[2] L. A. N. Amaral, A. Scala, M. Barthélemy, and H. E. Stanley, Proc. Natl. Acad. Sci. USA **97**, 11149 (2000).
[3] S. Boccaletti, V. Latora, Y. Moreno, M. Chavez, and D.-U. Huang, Phys. Rep. **424**, 4 (2006).
[4] L. M. Pecora and T. L. Carroll, Phys. Rev. Lett. **80**, 2109 (1998).
[5] Y.-Y. Liu, J.-J. Slotine, and A.-L. Barabási, Nature (London) **473**, 167 (2011).
[6] Z. Yuan, C. Zhao, Z. Di, W.-X. Wang, and Y.-C. Lai, Nat. Commun. **4**, 2447 (2013).

[7] Y.-Y. Liu and A.-L. Barabási, Rev. Mod. Phys. **88**, 035006 (2016).
[8] T. Gross and B. Blasius, J. R. Soc. Interface **5**, 259 (2008).
[9] W.-J. Yuan, J.-F. Zhou, Q. Li, D.-B. Chen, and Z. Wang, Phys. Rev. E **88**, 022818 (2013).
[10] C. Zhou and J. Kurths, Phys. Rev. Lett. **96**, 164102 (2006).
[11] Q. Ren and J. Zhao, Phys. Rev. E **76**, 016207 (2007).
[12] F. Sorrentino, Phys. Rev. E **80**, 056206 (2009).
[13] J.-F. Zhu, M. Zhao, W. Yu, C. Zhou, and B.-H. Wang, Phys. Rev. E **81**, 026201 (2010).
[14] W.-J. Yuan and C. Zhou, Phys. Rev. E **84**, 016116 (2011).
[15] F. Sorrentino and E. Ott, Phys. Rev. Lett. **100**, 114101 (2008).
[16] B. Ravoori, A. B. Cohen, A. V. Setty, F. Sorrentino, T. E. Murphy, E. Ott, and R. Roy, Phys. Rev. E **80**, 056205 (2009).
[17] X. F. Wang and G. Chen, Physica A (Amsterdam) **310**, 521 (2002).
[18] X. Li, X. Wang, and G. Chen, IEEE Trans. Circuit Syst. **51**, 2074 (2004).
[19] J. A. Almendral, I. Sendiña-Nadal, D. Yu, I. Leyva, and S. Boccaletti, Phys. Rev. E **80**, 066111 (2009).
[20] R. Gutiérrez, I. Sendiña-Nadal, M. Zanin, D. Papo, and S. Boccaletti, Sci. Rep. **2**, 396 (2012).
[21] L. Wang, H. P. Dai, H. Dong, Y. Y. Cao, and Y. X. Sun, Eur. Phys. J. B **61**, 335 (2008).
[22] J. Zhou, J.-A. Lu, and J. Lü, Automatica **44**, 996 (2008).
[23] K. Natori and K. Ohnishi, IEEE Trans. Ind. Electron. **55**, 5 (2008).
[24] J. Lu and D. W. C. Ho, Nonlin. Anal.: Real World Appl. **12**, 1974 (2011).
[25] A. E. Motter, C. S. Zhou, and J. Kurths, Europhys. Lett. **69**, 3 (2005).
[26] T. Nishikawa, A. E. Motter, Y.-C. Lai, and F. C. Hoppensteadt, Phys. Rev. Lett. **91**, 014101 (2003).
[27] O. E. Rössler, in *Synergetics (a workshop)*, edited by H. Haken (Springer, Berlin, 1977), p. 184.
[28] B. Blasius, A. Huppert, and L. Stone, Nature (London) **399**, 354 (1999).
[29] E. N. Lorenz, J. Atmos. Sci. **20**, 130 (1963).
[30] M. C. Mackey and L. Glass, Science **197**, 4300 (1977).
[31] I. Rojas, H. Pomares, J. L. Bernier, J. Ortega, B. Pino, F. J. Pelayo, and A. Prieto, Neurocomputing **42**, 267 (2002).
[32] A.-L. Barabási and R. Albert, Science **286**, 509 (1999).